PERGAMON

International Journal of Heat and Mass Transfer 42 (1999) 3205–3216

International Journal of HEAT and MASS TRANSFER

Heat transfer in crossflow regenerators

J.J. Saastamoinen*

VTT Energy, Box 1603, 40101 Jyväskylä, Finland

Received 30 December 1997; received in revised form 8 December 1998

Abstract

Heat transfer in regenerators when the hot and the cold gases flow alternatively and in crossflow directions through the material space is investigated. Exact analytical solutions for the temperatures of gases and solid material as function of time and space are presented for the general asymmetric and unbalanced case. The solutions can readily be used to dimension the regenerator operating in the crossflow mode. In cyclic stationary regenerators the gas outlet temperature varies with time and the damping of the temperature fluctuations is discussed. Applications in combustion of fuels with low heating value are presented. © 1999 Elsevier Science Ltd. All rights reserved.

1. Introduction

Different calculation methods for heat and mass transfer in packed beds and regenerators have been presented and reviewed in the literature [1–6]. Rotating regenerators are used in connection with gas turbines, ventilation systems and boilers to recover heat from exhaust gases to preheat the inlet air or gas. Fixed bed regenerators are used in many high temperature industrial processes and furnaces to recover heat from exhaust gases. The regenerator is also an essential part in the Stirling engine process. The use of a fixed bed regenerator in connection with a steam boiler can have many advantages [7]. It gives a means to raise the temperature uniformly inside the chamber, which enhances and smooths the thermal field while significantly reducing the temperature of the waste gases. In high temperature processes with regenerative burners the thermal NO formation can be suppressed by reducing peak temperatures using flue gas circulation [8–11] and great fuel savings can be achieved [11–15].

Regenerators are usually operating in the counterflow mode. Numerous methods to calculate the effectiveness of regenerators in counterflow have been presented in the literature [2]. An analytical approximate solution with high accuracy for the symmetric and balanced regenerator operating in counterflow has been developed [16]. Later the solution was generalized to the asymmetric and unbalanced regenerator [17]. The operation of regenerators in parallel flow has also been considered [2,18]. Heat and mass transfer in crossflow with a silica gel as adsorbent in the solid desiccant dehumidifier has been studied [19]. In the present paper, the operation of a crossflow regenerator as a heat exchanger is analysed.

The crossflow operation of recuperative heat exchangers and the connection of these units in series is frequently applied due to the easier manufacture. Arranging fluid flow in crossflow is easier than in counterflow, which could be especially useful in the design of regenerative burners. For the same reason, the crossflow mode could also be an interesting alternative for regenerators. The valve system to achieve the cyclic

---

* Tel.: +358-14-672-547; fax: +358-14-672-596.

E-mail address: jaakko.saastamoinen@vtt.fi (J.J. Saastamoinen)

0017-9310/99/$ - see front matter © 1999 Elsevier Science Ltd. All rights reserved.
PII: S0017-9310(99)00012-5

Nomenclature

c	specific heat [J kg^{-1} K^{-1}]
C	heat capacity, $C = c_s m_s$ [J K^{-1}]
$\dot{C}$	heat capacity flow rate, $\dot{C} = c\dot{m}$ [W K^{-1}]
G	conductance, $G = h_e S$ [W K^{-1}]
h	heat transfer coefficient [W m^{-2} K^{-1}]
H	heat of combustion or vaporization [J kg^{-1}]
L	length [m]
m	mass [kg]
$\dot{m}$	mass flow rate [kg s^{-1}]
R	ratio of heat capacity flow rates, $R = \dot{C}_{g,min}/\dot{C}_{g,max}$
S	heat transfer area of a regenerator sector [m^2]
t	time [s]
T	temperature [K]
u	moisture content, mass of water/dry mass
w	velocity [m s^{-1}]
x	coordinate along gas flow [m]
Z	dimensionless conductance, $Z = G_t/\dot{C}_{g,min}$.

Greek symbols

γ	ratio of heat capacities inside the heat storage, $\gamma = C_g/C_s$
ε	thermal effectiveness
ζ	dimensionless coordinate, $\zeta_i = G_t x_i/\dot{C}_{gi} L_i$
η	dimensionless time, $\eta_i = \Pi_i t/t_i$
η_C	combustion efficiency
θ	dimensionless temperature of solid, $\theta = (T_s - T_{g0,1})/(T_{g0,2} - T_{g0,1})$
ϑ	dimensionless temperature of gas, $\vartheta = (T_g - T_{g0,1})/(T_{g0,2} - T_{g0,1})$
Λ	dimensionless length, $\Lambda = G/\dot{C}_g$
ξ	dimensionless coordinate along the gas flow, $\xi_i = \Lambda_i x_i/L_i$
Π	dimensionless time period of a stage, $\Pi_i = G_i t_i/C_{si}$
Φ	heat flow [W]
ω	dimensionless frequency, $\omega = 2\pi/\Pi_p$.

Subscripts

a	outlet time average mixing
e	effective
F	furnace gas
f	fuel
g	gas, fluid
i	stage under consideration ($i = 1$ or $i = 2$)
j	stage not under consideration ($j = 1$ when $i = 2$, and $j = 2$ when $i = 1$)
m	mixing
max	greater
min	smaller
p	total period including stages 1 and 2
s	solid
t	total
w	water
0	inlet
1	cooling stage of solids
2	heating stage of solids.

operation is easier to accomplish in the crossflow mode. The effectiveness of a regenerator operating in crossflow is less than that of a counterflow regenerator. High effectiveness can be obtained by connecting crossflow regenerators in series and by arranging gas flow in counterflow. In a fixed crossflow regenerator, the gas flows periodically in perpendicular directions through the solid matrix as presented in Fig. 1. The valves are closed and opened cyclically. The advantage of rotating regenerators is the constant outlet mixing temperature. It is also possible to construct a rotating regenerator operating in the crossflow mode. One of the flows enters the regenerator through an annular duct. The other flow is directed in perpendicular direction and it leaves through the inner duct of the annulus. The valves remain closed now and the cyclic operation is obtained by rotating the heat storage matrix. Instead of rotating the matrix, it could be possible to rotate the valves to obtain periodic heat exchange between the two flows. The heat transfer in crossflow operation is analysed and analytical solutions for the transient temperature distributions and thermal effectiveness are derived in this paper.

The use of a regenerator in connection with combustion is illustrated in Fig. 2. When the heating value of the fuel is low, the combustion temperature becomes low and emissions as unburnt gases increase. Such fuels are for example moist fuels (wood, bark and sludges). The emission of volatile organic compounds diluted in air is an extreme case of a fuel with low caloric heating value. Regenerators are also used in the destruction of volatile organic compounds [12–14] and the combustion temperature can be decreased by catalytic combustion. The theoretical adiabatic combustion temperature may become too low to sustain stable combustion with such fuels. By using the heat recovery arrangement (Fig. 2) higher temperatures can be reached. The great carbon monoxide and hydrocarbon emissions when using wet fuels are usually due to the low combustion temperature. Water vapour itself in the atmosphere enhances the rate of oxidation of carbon monoxide [20]. Then excess air can be chosen lower with wet fuels, if high enough gas temperature is reached with the use of a regenerator. Besides the more efficient combustion, the air volume rate and fan power can be decreased and the efficiency of the combustor improved. The regenerator can also be a means to attain the high combustion temperatures that are required in the destruction of many toxic compounds.

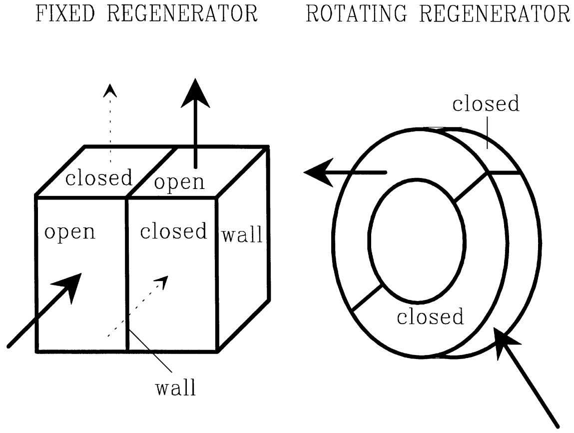

Fig. 1. Schematic of crossflow regenerator.

2. Equations describing heat transfer

The usual simplifying assumptions generally applied in the regenerator analysis are used in the mathematical model for the heat transfer phenomena. The heat is transferred between the gas and the surface of the solid elements locally by convection. The heat exchange between the surface and the interior of the solid takes place by conduction. The effect of the resistance of thermal conduction inside the solid elements is taken into account by using the effective heat transfer coefficient $h_e = h/(1+2\ Bi\ \phi)$. Bi is the Biot number and the coefficient ϕ describes the thermal resistance due to heat conduction in the solid element. It depends on the shape of the solid elements of the heat storage matrix [2]. It is approximately 1/6, 1/8 and 1/10 for plates, cylinders and spheres, respectively. Heat transfer by conduction, radiation and gas mixing in the flow direction are assumed to be negligible compared to the convective heat transported by the gas

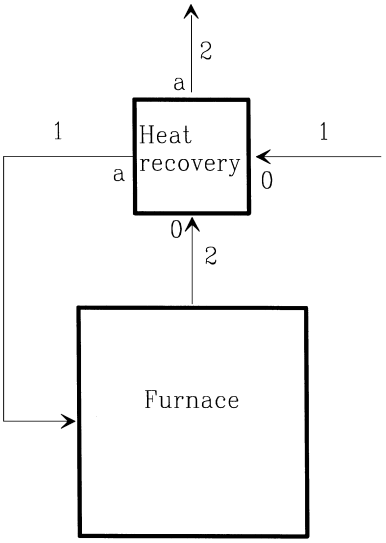

Fig. 2. Use of a regenerator as combustion air preheater.

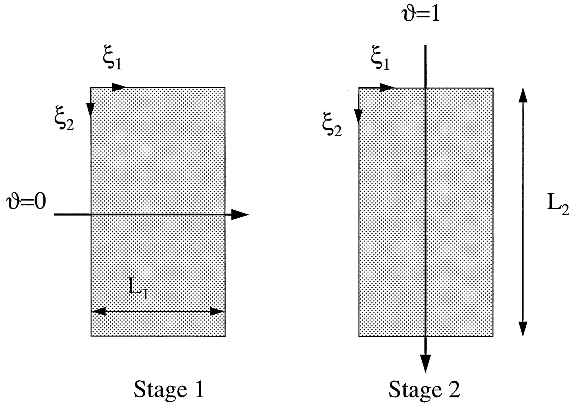

Fig. 3. The flow arrangement of gas through solid matrix in different stages in crossflow.

flow. The average heat transfer coefficients are used for the heating and cooling phases. However, allowances are made in the analysis for heat transfer coefficients, heat capacity flow rates and heat capacities to be different for the separate phases. The flow is assumed to be distributed evenly to the whole cross-sectional flow area. A construction that consists of several sectors, one of which is in the cooling (or heating) stage and the rest in the heating (or cooling) stage is an example of a crossflow regenerator with different heat capacities during different phases.

The heat exchange between gas and the solid heat storage matrix and the coordinate system is illustrated in Fig. 3. The gas flows through the heat storage in perpendicular direction during the two stages. The heat transfer in the gas and in the solid is described by the partial differential equations

$$\frac{\partial \vartheta}{\partial \xi_i} + \gamma \frac{\partial \vartheta}{\partial \eta_i} = \theta - \vartheta, \quad \frac{\partial \theta}{\partial \eta_i} = \vartheta - \theta \tag{1}$$

in dimensionless form for stages $i=1$ and $i=2$. The effect of the gas heat storage is small and in the analysis it is assumed that $\gamma = 0$. The dimensionless temperature scale is chosen so that

$$\vartheta(0,\xi_2,\eta_1) = \vartheta_{0,1} = 0 \text{ for stage 1}$$

$$\vartheta(\xi_1,0,\eta_2) = \vartheta_{0,2} = 1 \text{ for stage 2} \tag{2}$$

In cyclic operation the temperature distribution at the start of the stage 1 is the same as the distribution at the end of the stage 2. In addition, the temperature distribution at the start of the stage 2 is the same as the distribution at the end of the stage 1. Thus we have the initial conditions in cyclic operation

$$\begin{aligned} \theta(\xi_1,\xi_2,\eta_1 = 0) &= \theta(\xi_1,\xi_2,\eta_2 = \Pi_2) \\ \theta(\xi_1,\xi_2,\eta_2 = 0) &= \theta(\xi_1,\xi_2,\eta_1 = \Pi_1) \end{aligned} \tag{3}$$

3. Solution of equations in cyclic state

The Laplace transform with respect to the space coordinate is applicable for the study of both parallel flow and crossflow arrangements, since there is no change in the flow direction as in the counterflow. The Laplace transform

$$\bar{f}(s_i) = \int_0^\infty \mathrm{e}^{-s_i \xi_i} f(\xi_i)\, \mathrm{d}\xi_i \tag{4}$$

is applied with respect to coordinates ξ_i twice in succession. The partial differential equations reduce to the equations

$$s_i \bar{\vartheta} - \frac{\vartheta_{0,i}}{s_j} = \bar{\theta} - \bar{\vartheta} \quad \frac{\mathrm{d}\bar{\theta}}{\mathrm{d}\eta_i} = \bar{\vartheta} - \bar{\theta} \tag{5}$$

The transformed temperatures are indicated by the bar. The solution of the equations for transformed solid temperatures is

$$\bar{\theta} = \bar{\theta}_i \exp\left(- \frac{s_i \eta_i}{1 + s_i} \right) + \frac{\vartheta_{0,i}}{s_i s_j} \left[1 - \exp\left(- \frac{s_i \eta_i}{1 + s_i} \right) \right] \tag{6}$$

The initial temperature distributions, the temperature distributions at the start of the stages $i=1$ and $i=2$, can readily be solved by applying the cyclic initial conditions. The result is

$$\boxed{\bar{\theta}_i = \frac{1}{s_i s_j} \frac{\vartheta_{0,i} \exp\left(- \frac{s_j \Pi_j}{1 + s_j} \right) \left[1 - \exp\left(- \frac{s_i \Pi_i}{1 + s_i} \right) \right] + \vartheta_{0,j} \left[1 - \exp\left(- \frac{s_j \Pi_j}{1 + s_j} \right) \right]}{1 - \exp\left(- \sum_{k=1}^{2} \frac{s_k \Pi_k}{1 + s_k} \right)}} \tag{7}$$

The denominator of the Eq. (7) can be expanded as

$$\left[1 - \exp\left(- \sum_{k=1}^{2} \frac{s_k \Pi_k}{1 + s_k} \right) \right]^{-1} = \sum_{n=0}^{\infty} \exp\left(- \sum_{k=1}^{2} \frac{n s_k \Pi_k}{1 + s_k} \right) \tag{8}$$

by using the MacLaurin series $1/(1-x)=1+x+x^2+x^3 \ldots$ This is applied to the transformed solutions for solid temperature (6) and corresponding formula for gas temperature. The inversion can be performed term by term using the inverse Laplace transforms

$$L^{-1}\left(\frac{1}{s}\,\mathrm{e}^{-\frac{s\eta}{1+s}}\right)=G(\eta,\xi)$$

$$L^{-1}\left(\frac{1}{s(1+s)}\,\mathrm{e}^{-\frac{s\eta}{1+s}}\right)=1-G(\xi,\eta) \tag{9}$$

Several expressions for the function $G(x,y)$ and its integral function have been presented [21–30] and their properties have been discussed earlier [27,28]. Luo suggested the following formulas [29]

$$G(x,y)=\mathrm{e}^{-x-y}\sum_{j=1}^{\infty}\frac{y^j}{j!}\sum_{k=0}^{j}\frac{x^k}{k!}$$

$$\begin{aligned} G_1(x,y)&=\int_0^y G(x,u)\,\mathrm{d}u \\ &=\mathrm{e}^{-x-y}\sum_{j=1}^{\infty}\frac{y^j}{j!}\sum_{k=0}^{j-1}(j-k)\frac{x^k}{k!} \end{aligned} \tag{10}$$

The temperatures in single-blow operating mode of a heat storage can be expressed by using the function $G(x,y)$; useful approximations for large x and y have been presented in the literature [3,28,29].

The temperature distribution of the solid for stage i is

$$\begin{aligned} \theta=\vartheta_{0,i}-(-1)^i\sum_{n=0}^{\infty}&[G(n\Pi_j,\xi_j) \\ &-G((n+1)\Pi_j,\xi_j)]G(\eta_i+n\Pi_i,\xi_i) \end{aligned} \tag{11}$$

where $j=2$ when $i=1$, and $j=1$ when $i=2$. The gas temperature distribution is

$$\begin{aligned} \vartheta=\sum_{n=0}^{\infty}&[G(n\Pi_j,\xi_j)-G((n+1)\Pi_j,\xi_j)] \\ &\times[1-\vartheta_{0,i}+(-1)^iG(\xi_i,\eta_i+n\Pi_i)] \end{aligned} \tag{12}$$

The time dependent average (mixing) gas outlet temperature from the regenerator is obtained by integrating Eq. (12)

$$\begin{aligned} \vartheta_{\mathrm{m}}=\frac{1}{\Lambda_j}\sum_{n=0}^{\infty}&[G_1(n\Pi_j,\Lambda_j)-G_1((n+1)\Pi_j,\Lambda_j)] \\ &\times[1-\vartheta_{0,i}+(-1)^iG(\Lambda_i,\eta_i+n\Pi_i)] \end{aligned} \tag{13}$$

The effectiveness of the crossflow regenerator is defined in the usual way as the average temperature increase or decrease of the fluid in the regenerator during stage i divided by the difference between the inlet temperatures

$$\begin{aligned} \varepsilon_i&=\frac{\Delta T_{\mathrm{g},i}}{T_{\mathrm{g}0,2}-T_{\mathrm{g}0,1}} \\ &=\vartheta_{0,i}-\frac{(-1)^i}{\Pi_i\Lambda_j}\int_0^{\Pi_i}\int_0^{\Lambda_j}\vartheta(\xi_i=\Lambda_i,\xi_j,\eta_i)\,\mathrm{d}\xi_j\,\mathrm{d}\eta_i \end{aligned} \tag{14}$$

It can be deduced from the energy balances for the stages that the effectiveness of the two stages are related to each other by the equation

$$\varepsilon_2=\frac{\Lambda_2\Pi_1}{\Lambda_1\Pi_2}\varepsilon_1 \tag{15}$$

The greater of the effectiveness values that is related to the smaller heat capacity flow rate is usually defined as the effectiveness of the heat exchanger. The effectiveness which is identical to the previous one can also be calculated as the ratio heat energy stored in or charged from the solids divided by the total energy brought to the regenerator during the stage i,

$$\begin{aligned} \varepsilon_i=\frac{C_i\Delta T_{\mathrm{s},i}}{\dot{C}_i(T_{\mathrm{g}0,2}-T_{\mathrm{g}0,1})}&=\frac{(-1)^{1+i}}{\Pi_i\Lambda_j}\int_0^{\Lambda_2}\int_0^{\Lambda_1} \\ &\times[\theta(\xi_1,\xi_2,\eta_i=0)-\theta(\xi_1,\xi_2,\eta_i=\Pi_i)]\,\mathrm{d}\xi_1\,\mathrm{d}\xi_2 \end{aligned} \tag{16}$$

By substituting Eq. (11) into Eq. (16) and by integrating the effectiveness becomes

$$\begin{aligned} \varepsilon_i=\frac{1}{\Pi_i\Lambda_j}\sum_{n=0}^{\infty}\prod_{k=1}^{2}&[G_1(n\Pi_k,\Lambda_k) \\ &-G_1((n+1)\Pi_k,\Lambda_k)] \end{aligned} \tag{17}$$

In the special case of a balanced and symmetric regenerator, $\Lambda_1=\Lambda_2$ and $\Pi_1=\Pi_2$, this is simplified into

$$\varepsilon=\frac{1}{\Pi\Lambda}\sum_{n=0}^{\infty}[G_1(n\Pi,\Lambda)-G_1((n+1)\Pi,\Lambda)]^2 \tag{18}$$

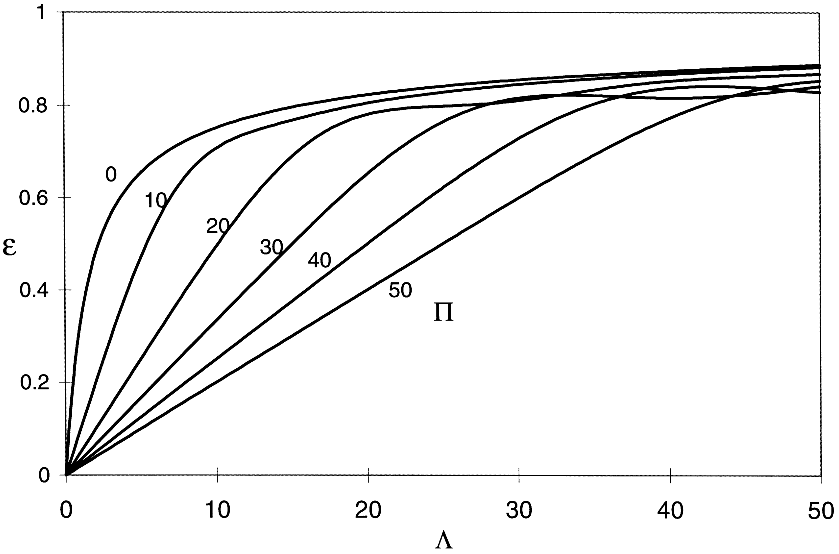

Fig. 4. Effectiveness of symmetric and balanced crossflow regenerator.

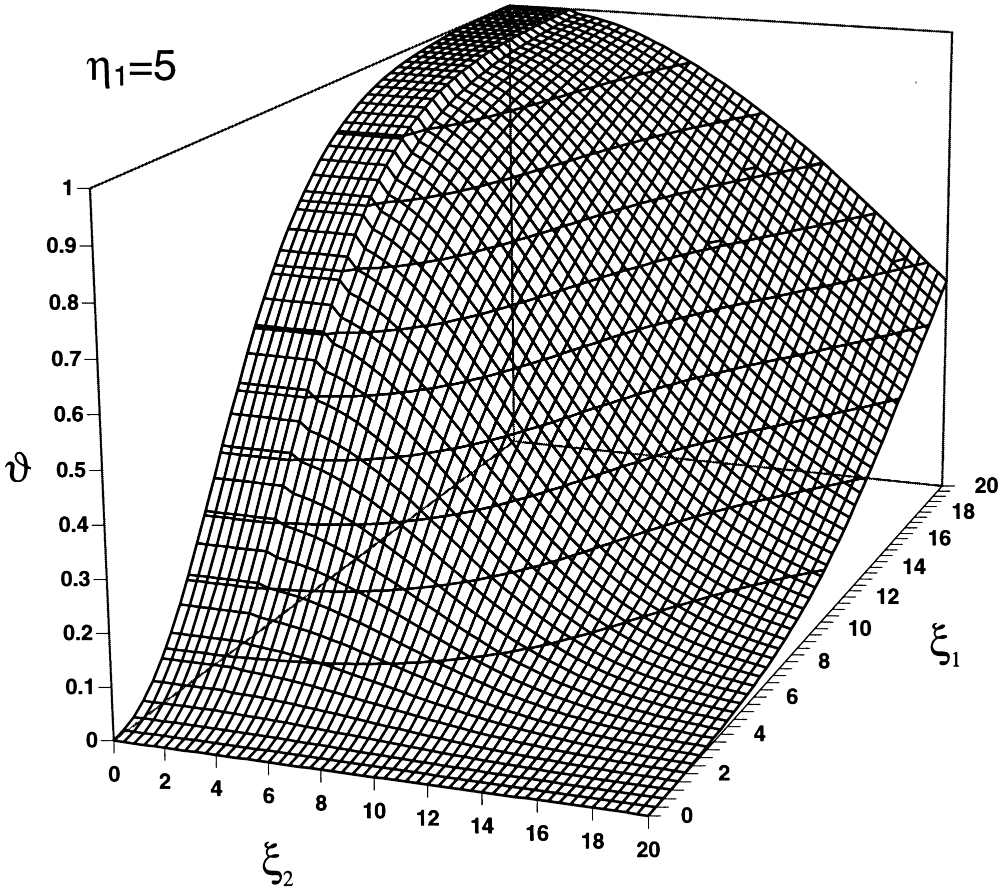

Fig. 5. Normalized gas temperature distribution inside a symmetric and balanced crossflow regenerator ($\Pi = 10$, $\Lambda = 20$) at time $\eta_1 = 5$.

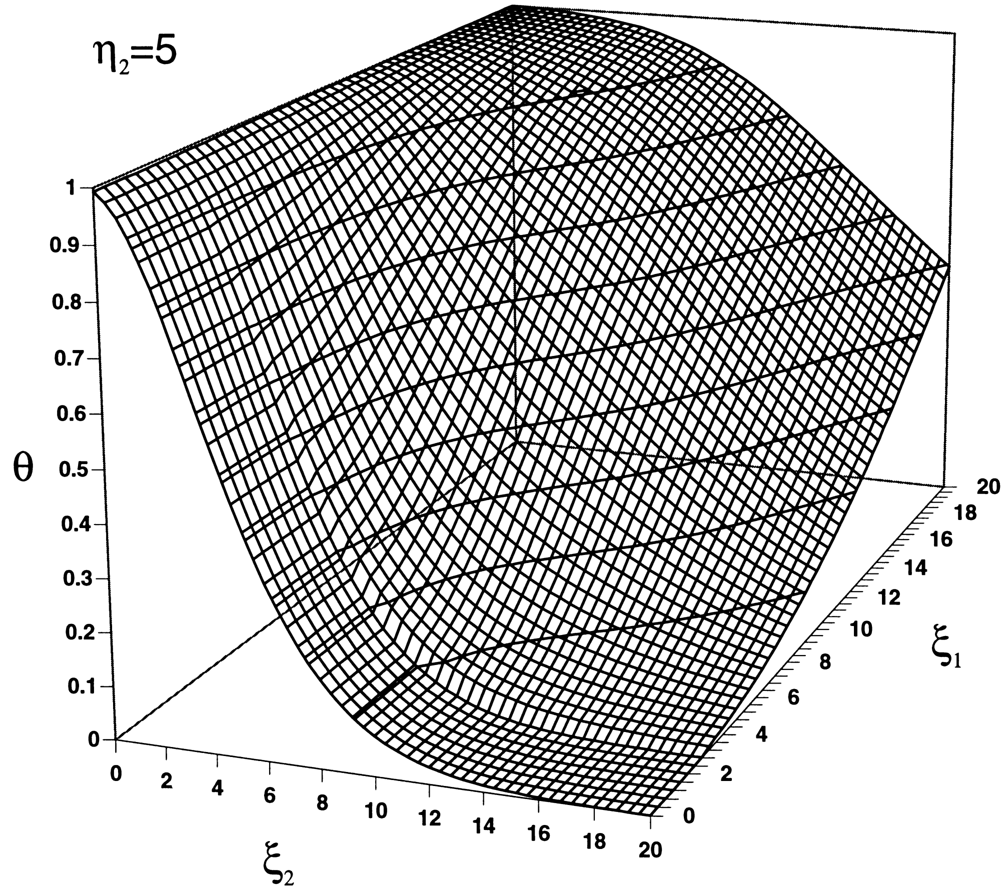

Fig. 6. Normalized solid temperature distribution inside a symmetric and balanced crossflow regenerator ($\Pi=10$, $\Lambda=20$) at time $\eta_2=5$.

4. Discussion

4.1. Temperatures and effectiveness

The effectiveness of a parallel flow regenerator reaches a maximum with a certain value of Λ [2]. Such maximum does not exist for the counterflow mode, where the effectiveness always increases with increasing Λ. The behaviour of the crossflow regenerator is somewhat between these two cases. The effectiveness of the balanced and symmetric regenerator is presented in Fig. 4. It is seen that for large values of Π effectiveness reaches a maximum with a specific heat transfer area. For example, when $\Pi=30$, the maximum effectiveness is obtained when $\Lambda=33$. Such maximum effectiveness does not exist for small values of Π, but effectiveness is increasing monotonously with increasing Λ. The efficiency in crossflow is less than in counterflow. Higher total effectiveness for the heat recovery can be obtained by connecting two or more crossflow regenerators in series in counterflow. The thermal operation is illustrated by the calculated temperature distributions in gas and solid for the symmetric and balanced regenerator ($\Pi=\Pi_1=\Pi_2=10$, $\Lambda=\Lambda_1=\Lambda_2=20$). The dimensionless temperature distributions for the gas and the solids are shown in Figs. 5 and 6 as illustrations. Two-dimensional temperature waves in the gas and in the solids propagate in the directions of the gas flows. Also the gas temperature distribution as function of ξ_2 at the moment $\eta_1=5$ at the outlet ($\xi_1=\Lambda_1=20$) can be seen. The average gas outlet temperature variation is shown in Fig. 8 for several cases.

The dimensioning of a heat exchanger is a typical techno-economical optimisation problem [30]. The crossflow arrangement is especially attractive compared to counterflow in applications, where the heat capacity flow rates differ from each other, since the flow areas can be chosen to be unequal, which is beneficial for the optimisation of both the heat transfer and the pressure losses. An example of such an application is the use of a regenerator as the preheater for recircu-

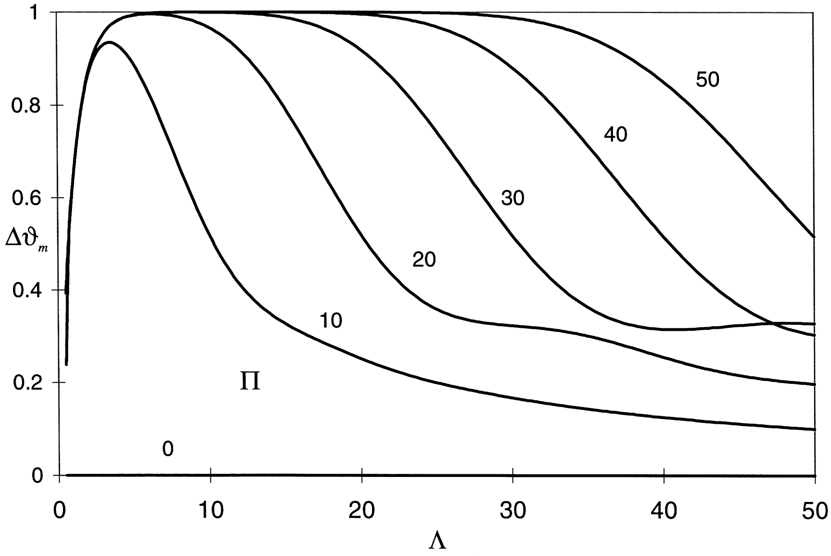

Fig. 7. Difference between average gas outlet temperatures at the start and at the end of a stage for symmetric and balanced crossflow regenerators.

lated flue gas in a furnace to reduce the NO formation, where only a part of the flue gas is reheated and returned to the furnace. Also in combustion of wet biomass, the heat capacity flow rates of combustion air and flue gas become different. In the situation, where the heat capacity flow rates are different, the effectiveness related to the flow with lower heat capacity flow rate can reach a high value; for example $\varepsilon_1 = 0.944$ for the case (d) in Fig. 8. In this case, use of the thermally most efficient counterflow arrangement instead of crossflow can only slightly improve the effectiveness.

In heat storage applications with a single storage the charging time can be long, but the discharge of the heat takes place in a shorter time or vice versa. Then also the mass flow rates can be different and the cross-sectional areas can be optimized regarding both heat transfer and pressure losses.

4.2. Limiting case $\Pi \rightarrow 0$

In the limiting case, when the cycle period approaches zero ($\Pi \rightarrow 0$), the temperature distribution and the efficiency of counterflow regenerators approach those of corresponding recuperative heat exchanger [2]. This is also the case in connection with the crossflow operation. In this limiting case the heat exchange between the fluid flows is described by the partial differential equations

$$\frac{\partial \vartheta_1}{\partial \zeta_1} = \vartheta_2 - \vartheta_1 \quad \frac{\partial \vartheta_2}{\partial \zeta_2} = \vartheta_1 - \vartheta_2 \tag{19}$$

in dimensionless form. After the early work [21,22] several exact formulas using complicated functions for calculating the effectiveness of crossflow heat exchangers have been presented [23]. The different solutions presented in the literature are basically identical, since they are exact solutions of the same equations obtained by different methods and can be expressed as

$$\theta_1 = 1 - G(\zeta_1, \zeta_2) \tag{20}$$

$$\theta_2 = G(\zeta_2, \zeta_1) \tag{21}$$

The effectiveness of crossflow heat exchanger is found by calculating the average fluid temperature at the outlet. The well-known result is

$$\varepsilon = 1 - \frac{1}{RZ} G_1(Z, RZ) = \frac{1}{R} - \frac{1}{RZ} G_1(RZ, Z) \tag{22}$$

The Eqs. (20) and (21) can also be used to calculate the response of gas and solid temperatures in a fixed bed to a step change in the gas inlet temperature [24–26], since the governing equations are analogous to the Eqs. (19) of the crossflow heat exchanger. In this case θ_1 and θ_2 denote the temperatures of the solid and fluid, respectively, $\theta_1(\eta = 0) = 0$, the dimensionless time $\zeta_1 = G(t - x/w)/C$ and ζ_2 is the dimensionless coordinate along the flow.

4.3. Means to damp the cyclic outlet temperature

In stationary fixed bed regenerators the outlet mixing temperature is varying with time during the cycle. The difference between outlet temperatures at the start

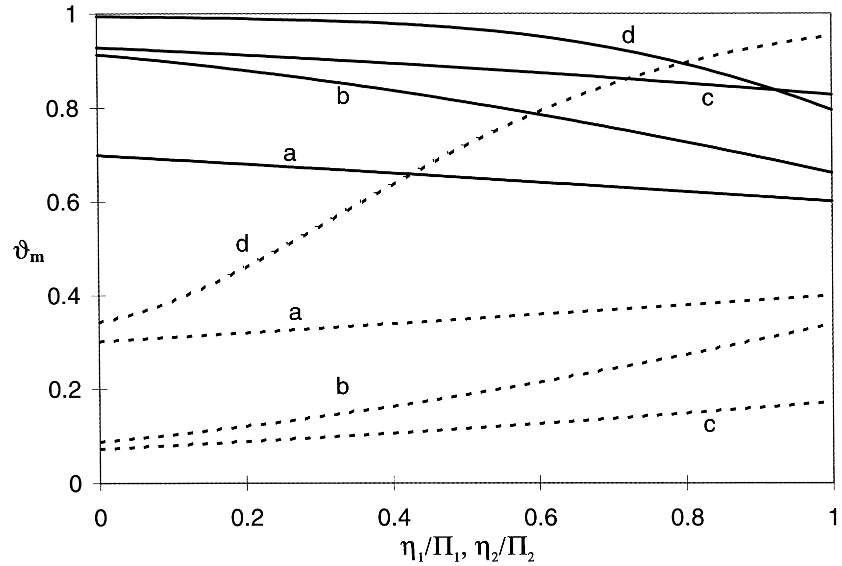

Fig. 8. Normalized average (mixing) outlet temperature of gas as a function of time during stages 1 and 2 in several cases: (a) $\Pi_1 = \Pi_2 = 1$, $\Lambda_1 = \Lambda_2 = 5$; (b) $\Pi_1 = \Pi_2 = 10$, $\Lambda_1 = \Lambda_2 = 20$; (c) $\Pi_1 = \Pi_2 = 10$, $\Lambda_1 = \Lambda_2 = 50$; (d) $\Pi_1 = \Pi_2 = 10$, $\Lambda_1 = 15$, $\Lambda_2 = 5$.

and at the end of a stage for symmetric and balanced regenerators is shown in Fig. 7. In a massive system, for example a furnace with massive walls, this does not necessarily have a great effect on the operating temperature. In some cases, this temperature variation can be disadvantageous. A fixed bed can be used as a gas temperature damper. The complete damping of the sine term is illustrated in Fig. 9. The heat transfer in the fixed bed can be described by Eq. (1) in which $i = 1$, since there is only one flow direction. The use of the Laplace transform and a simple frequency response analysis gives the response at the outlet

$$\vartheta = \exp\left(-\frac{\omega^2\Lambda}{1+\omega^2}\right)\sin\left(\omega\eta - \gamma\omega\Lambda - \frac{\omega\Lambda}{1+\omega^2}\right) \quad (23)$$

to a sinusoidal gas inlet temperature $\vartheta = \sin(\omega\eta)$. In order to achieve complete damping, the fixed bed is

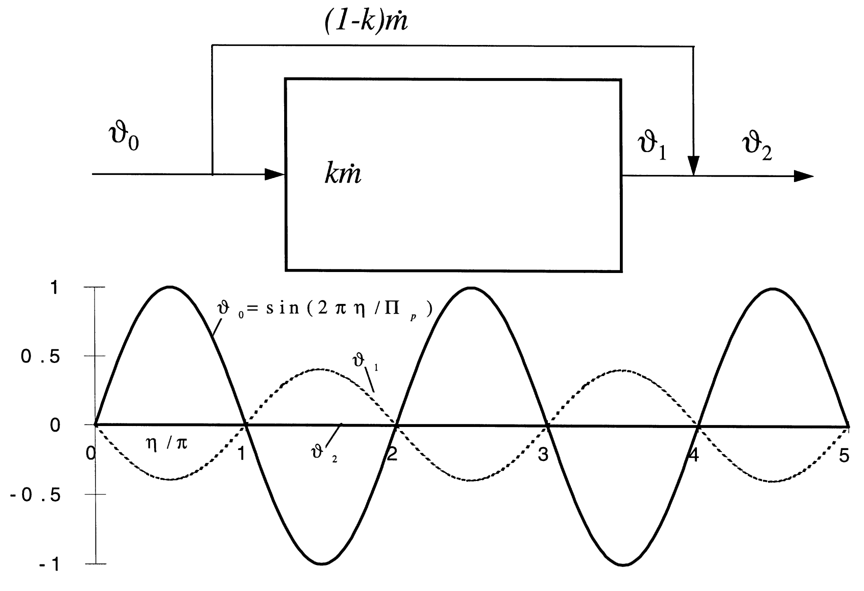

Fig. 9. A fluid temperature damper.

dimensioned to have a phase lag of a half period, $\vartheta_1 = \sin(\omega\eta - \pi)$, and we obtain

$$\Lambda = h_e S/(k\dot{m}_g c_g) = \frac{\pi(\omega + 1/\omega)}{1 + \gamma(1 + \omega^2)} \tag{24}$$

where $\gamma \approx 0$ for gases. The total damping is obtained when the mass flow ratio is chosen as

$$k = \left[1 + \exp\left(-\frac{\pi\omega}{1 + \gamma(1 + \omega^2)}\right)\right]^{-1} \tag{25}$$

which is obtained by giving the value zero for the mixing temperature, $\vartheta_2 = (1-k)\vartheta_0 + k\vartheta_1 = 0$. A cyclic gas temperature variation can be presented as the Fourier series

$$\vartheta_0 = a_0/2 + \sum_{n=1}^{\infty}[a_n \cos(\omega_n\eta) + b_n \sin(\omega_n\eta)] \tag{26}$$

where $\omega_n = n\omega$. When the gas flows through the damper presented in Fig. 9, the first term $n = 1$ is totally damped. The outlet mixing temperature is

$$\begin{aligned}\vartheta_2 &= (1 - k)\vartheta_0 + k\vartheta_1 = a_0/2 + (1 - k)\\ &\times \sum_{n=2}^{\infty}[a_n \cos(\omega_n\eta) + b_n \cos(\omega_n\eta)] + k\\ &\times \sum_{n=2}^{\infty} e^{-\omega_n\varphi_n}[a_n \cos(\omega_n\eta - \gamma\omega_n\Lambda - \varphi_n)\\ &+ b_n \sin(\omega_n\eta - \gamma\omega_n\Lambda - \varphi_n)]\end{aligned} \tag{27}$$

where the phase lag $\varphi_n = \omega_n\Lambda/(1 + \omega_n^2)$. It is also possible to connect two or more regenerators parallel in series operating with shifted stages to reduce the temperature variation; then the variation of the outlet mixing temperature becomes smaller. It is also possible to divide the regenerator in several channels filled with the heat storage material so that the adjacent channels are in crossflow and operated with a phase lag so that the system corresponds to two or more regenerators in series resulting in a smaller amplitude and phase shift in the outlet gas temperature. The use of a bypass is also a means to regulate the outlet temperature. In combustion systems the temperature variation can in some cases also be damped by modulating the fuel rate (combustion rate), air rate, O_2 content of oxidizer gas (the degree of flue gas recirculation) or furnace cooling rate cyclically.

4.4. Illustrative examples

The use of a regenerator in connection with combustion (Fig. 2) is considered as an illustration here. The inlet and outlet temperatures of the combustion chamber and the regenerator can be solved from simple thermal balances

$$T_{ga,1} = \frac{(1 - \varepsilon)\dot{C}_{F2}T_{g0,1} + \varepsilon[(\dot{C}_{F2} - \dot{C}_{F1})T_f + \eta_C\dot{m}_f H_f - \Phi]}{\dot{C}_{F2} - \varepsilon\dot{C}_{F1}}$$

$$T_{g0,2} = \frac{(1 - \varepsilon)\dot{C}_{F1}T_{g0,1} + (\dot{C}_{F2} - \dot{C}_{F1})T_f + \eta_C\dot{m}_f H_f - \Phi]}{\dot{C}_{F2} - \varepsilon\dot{C}_{F1}}$$

$$T_{ga,2} = T_{g0,2} - \frac{\dot{C}_{g1}}{\dot{C}_{g2}}(T_{ga,1} - T_{g0,1}) \tag{28}$$

The entrance temperature of the fuel T_f to the system is chosen as the reference temperature for the heating value of the fuel. The specific heat c_{F2} for flue gas 2 in the furnace is the average in the temperature interval between T_f and $T_{g0,2}$. For the oxidizer gas 1 in the furnace c_{F1} is the average between T_f and $T_{ga,1}$. By the use of heat recovery ($\varepsilon > 0$) it is possible to reach higher combustion temperatures than the theoretical adiabatic combustion temperature for non-dissociating products ($\varepsilon = \Phi = 0$ and $\eta_C = 1$) even for a non-adiabatic case with heat losses $\Phi > 0$.

Two illustrations of fixed bed regenerators are considered. In these examples $\eta_C = 1$, $t_1 = t_2 = 300$ s. The regenerator consists of two parallelepiped ($L_1 \times L_2 \times L_3$) storages filled with sieved gravel, which consists of spherical stones 20 mm in diameter, $c = 800$ J kg^{-1}, density 2700 kg m^{-3} and heat conductivity 3.5 W m^{-1} K^{-1}) with porosity 37%. The effect of the inner thermal resistance of the solids reducing the effectiveness cannot be ignored in these cases, since Biot number ($Bi < 1$ in the examples) is not small enough due to the large diameter of the solids. Air with 0.6 wt.% H_2O ($T_{g0,1} = T_f = 298$ K) is used as the oxidizer gas.

Very diluted cool mixtures of methane and air can be combusted catalytically with the aid of a regenerator, which is considered as the first illustration. If methane emissions are converted to carbon dioxide and water vapour by combustion, net emission of greenhouse gases decreases, since energy from combustion may substitute some use of fossil fuels, and more importantly, since the greenhouse effect of methane is much greater than that of carbon dioxide. The gas released for example from landfills, municipal waste waters, marshlands and bottoms of lakes and sea bays is often of so high methane concentration that high enough combustion temperatures can be reached directly. For example, gas separated from bogs has directly been combusted for heating purposes in Finland over 60 years ago. However, methane from different sources, such as the houses for animals and manure storage for example, may be diluted in air so that direct combustion is impossible due to the low heating value. By ventilating the animal house and by enriching this gas by circulation in channels in the manure storage, the heating value could be increased. In the following example the methane is diluted with air so that the mixture (total mass flow rate 1.0 kg s^{-1}) contains 10 times more air than required in stoichiometric combustion. The theoretical adiabatic combustion temperature is as low as 570 K. Here the adiabatic combustion temperature 1300 K is chosen, but by catalytic combustion the temperature required to reach a high enough oxidation rate can be decreased. The regenerator effectiveness to reach this temperature level is $\varepsilon = 0.7626$ in the adiabatic case $\Phi = 0$ (Eq. 28). We choose the cross-section areas $A_1 = L_2 \times L_3 = 0.5$ m^2 and $A_2 = L_1 \times L_3 = 0.5$ m^2. Heat transfer coefficients were estimated from a correlation for fixed beds [31] and we get $\Pi_1 = 8.24$. The regenerator operation is almost symmetric and balanced in this case ($\Lambda_1/\Lambda_2 = 0.995 \approx 1$, $\Pi_1/\Pi_2 = 0.942 \approx 1$). By using Eq. (17), the required effectiveness can be obtained, when $\Lambda_1 = 11.78$, which corresponds to the heat transfer surface area 66 m^2, mass $m = 592$ kg and volume $V_t = 0.348$ m^3 of a single storage giving the dimensions $L_1 = 0.696$ m, $L_2 = 0.696$ m and $L_3 = 0.718$ m. If there is a simultaneous need for heat energy exceeding the 287 kW ($T_{ga,2} = 576$ K) obtained in the combustion of the gas emission, it is possible to reduce the regenerator size by introducing additional fuel in the furnace. In the non-adiabatic case, the required temperature level can be attained by increasing the regenerator size. The combustion reactivity of methane is rather low compared to many other gases. The temperature level required in catalytic combustion of organic compounds is between 550 and 800 K and CO can successfully be combusted at less than 600 K.

Combustion of wet fuel is considered as the second illustration. Landfill as a means to dispose industrial and municipal waste sludges is becoming expensive due to new legislation in many countries. Combustion can be an economic alternative of disposal and then also usable energy could be gained, but the direct combustion is difficult due to the great moisture content. Also the use of the energy from wet waste wood and bark for example in sawmills for drying of timber is difficult due to the low heating value of the fuel. In the following example combustion of wet wood 1.0 kg s^{-1} with moisture content $u = 3.5$ corresponding to only 22.2% dry material in the fuel is studied. The elemental composition of dry ash-free wood is 50% C, 6% H, 44% O, 0% N and S and the ash content is 0.5%. The lower heating value of the fuel is only 2.3 MJ kg^{-1}, when the heating value of dry wood is 18.88 MJ kg^{-1}, since it depends on the moisture content, $H_f = (H_{f,u=0} - uH_w)/(1+u)$. The mass flow rate of the exhaust gas 2 exceeds greatly the mass flow rate of the inlet air 1 due to the fuel and its moisture added in the furnace. In this case the regenerator operates in the asymmetric and unbalanced mode. Excess air is used and the stoichiometric coefficient 1.2 is assumed. The theoretical adiabatic combustion temperature is 926 K ($\varepsilon = 0$), which is too low to sustain stable combustion. The theoretical limiting adiabatic combustion temperature, when $\varepsilon = 1$, is 1374 K. When a regenerator with $\varepsilon = 0.8$ is applied the adiabatic combustion temperature 1241 K is reached. The heating power 2.29 MW obtained at exit temperature $T_{ga,2} = 921$ K, which is based on the lower heating value of the moist fuel, can greatly be increased by flue gas condensation, if the temperature level of the process (heating, drying), where the heat is used, is low. We choose the cross-sectional areas $A_1 = 0.5$ m^2 and $A_2 = 1.0$ m^2. It is found that $\Pi_1 = 10.57$, $\Pi_1/\Pi_2 = 1.069$ and $\Lambda_1/\Lambda_2 = 2.521$. The required effectiveness can be obtained, when $\Lambda_1 = 10.24$, which corresponds to the heat transfer surface area 70 m^2, the mass 633 kg and the volume 0.372 m^2 of the solids in a single storage. Thus, the dimensions of a single storage are $L_1 = 0.744$ m, $L_2 = 0.372$ m and $L_3 = 1.343$ m. In practice the combustion is not adiabatic due to heat losses and the combustion efficiency is less than 100%. The required regenerator effectiveness and dimensions can be estimated for this situation ($\eta_C < 1$, $\Phi > 0$) as well by using Eqs. (17) and (28). In case of disposal of waste sludges containing even less dry material or having even lower heating value the energy from combustion could be used to predry the sludge.

5. Concluding remarks

Analytical solutions for the temperature distributions and effectiveness of crossflow regenerators have been derived. As a special case, when the period length approaches zero, the problems reduce to that of the crossflow recuperative heat exchangers in steady state. The time-dependent outlet temperature from the fixed regenerator can be damped by a separate temperature damper or by using one or several regenerators in parallel with a phase time lag between them. Regenerators have been applied in the past and are applied at present in high temperature industrial processes and in power production. Regenerators can be applied in connection with energy production or destruction of waste materials by combustion, when the material to be combusted, such as diluted volatile organic compounds and methane, moist bark, wood and sludges, has a low heating value. Applications for regenerative heat exchangers can also be found in the new combustion and gasification concepts of solid fuels with flue gas circulation and possible oxygen enrichment.

Acknowledgements

The support from the Commission of the European Communities through contract JOR3-CT96-0059 and from Finnish National Combustion and Gasification Research Programme LIEKKI 2 are acknowledged.

References

[1] M. Jakob, in: Heat Transfer, vol. II, Wiley, New York, 1957, pp. 261–341.

[2] H. Hausen, in: Wärmeübertragung im Gegenstrom, Gleichstrom und Kreuzstrom, Springer-Verlag, Berlin, 1976, pp. 259–429.

[3] F.W. Schmidt, A.J. Willmott, Thermal Energy Storage and Regeneration, McGraw-Hill, New York, 1981.

[4] N. Wakao, S. Kaguei, Heat and Mass Transfer in Packed Beds, Gordon and Breach Science Publishers, New York, 1982.

[5] A.E. Saez, B.J. McCoy, Transient analysis of packed bed thermal storage systems, International Journal of Heat and Mass Transfer 26 (1983) 49–54.

[6] M. Riaz, Analytical solutions for single- and two-phase models of packed-bed thermal storage systems, ASME Journal of Heat Transfer 99 (1977) 489–492.

[7] A.K. Gupta, R. Tanaka, S. Mochida, T. Hasegawa, Excess enthalpy combustion in boilers and furnaces, in: Proceedings of 3rd European Conference on Industrial Furnaces and Boilers (INFUB), Lisbon, 1995, p. 16.

[8] J.A. Wünning, J.G. Wünning, Recuperative and regenerative burners using flameless oxidation, in: Proceedings of 3rd European Conference on Industrial Furnaces and Boilers (INFUB), Lisbon, 1995, p. 6.

[9] J.A. Wünning, J.G. Wünning, Flameless oxidation to reduce thermal NO-formation, Progress in Energy and Combustion Science 23 (1997) 81–94.

[10] M. Katsuki, T. Hasegawa The science and technology of combustion in highly preheated air. 27th Symposium (International) on Combustion, University of Colorado at Boulder, USA, 2–7 August 1998.

[11] Y. Suzukawa, Sh. Sugiyama, Y. Hino, M. Ishioka, I. Mori, Heat transfer improvement and NO_x reduction by highly preheated air combustion, Energy Conversion and Management 38 (1997) 1061–1071.

[12] F.E. Weinberg, Combustion in heat recirculating burners, in: F.E. Weinberg (Ed.), Advanced Combustion Methods, Academic Press, London, 1986, pp. 183–236.

[13] F.E. Weinberg, Combustion research for the 21st century—some speculative extrapolations, Combustion Science and Technology 98 (1994) 349–359.

[14] F. Weinberg, Heat-recirculating burners: principles and some recent developments, Combustion Science and Technology 121 (1996) 3–22.

[15] N.H. Malik, M.S. Saimbi, B.S. Sidhu, Regenerators—approaching the ultimate in heat recovery devices, in: Innovation in Process Energy Utilization, Hemisphere, New York, 1988, pp. 249–263.

[16] B.S. Baclic, The application of the Galerkin method to the solution of the symmetric and balanced counterflow regenerator problem, ASME Journal of Heat Transfer 107 (1985) 214–221.

[17] F.E. Romie, B.S. Baclic, Methods for rapid calculation of the operation of asymmetric counterflow regenerators, ASME Journal of Heat Transfer 110 (1988) 785–788.

[18] F.E. Romie, A solution for the parallel-flow regenerator, ASME Journal of Heat Transfer 114 (1992) 278–280.

[19] J-Y. San, Heat and mass transfer in a two-dimensional cross-flow regenerator with a solid conduction effect, International Journal of Heat and Mass Transfer 36 (1993) 633–643.

[20] C.K. Westbrook, F.L. Dryer, Simplified reaction mechanisms for the oxidation of hydrocarbon fuels in flames, Combustion Science and Technology 27 (1981) 31–43.

[21] W. Nusselt, Der wärmeübergang im kreuzstrom, Z. Ver. Deut. Ing. 71 (1911) 85–91.

[22] W. Nusselt, Eine neue formel für den wärmedurchgang im kreuzstrom, Technische Mechanik und Thermodynamik 1 (1930) 417–422.

[23] B.S. Baclic, P.J. Heggs, On the search for new solutions of the single-pass crossflow heat exchanger problem, International Journal of Heat and Mass Transfer 28 (1985) 1965–1976.

[24] T.E.W. Schumann, Heat transfer: a liquid flowing through a porous prism, J. Franklin Inst. 208 (1929) 405–416.

[25] A. Anzelius, Über erwärmung vermittels durchströmender medien, Z. Angew. Math. Mech. 6 (1926) 291–294.

[26] W. Nusselt, Die theorie des winderhitzers, Z. Ver. Deut. Ing. 71 (1927) 85–91.

[27] J. Łach, W. Pieczka, On the properties of some special functions related to Bessel's functions and their application in heat exchanger theory, International Journal of Heat and Mass Transfer 27 (1984) 2225–2238.

[28] F.E. Romie, Two functions used in the analysis of crossflow exchangers, regenerators, and related equipment, ASME Journal of Heat Transfer 109 (1987) 518–521.

[29] X. Luo, Theoretical investigation on cross-flow heat exchangers with axial dispersion in one fluid, in: R.K. Shah (Ed.), Compact Heat Exchangers for the Process Industries, Begell House, New York, 1997, pp. 417–423.

[30] P. Sarkomaa, Optimum economic dimensioning of an indirect heat-exchanger, Acta Polytechnica Scandinavica, Mechanical Engineering Series 76 (1979) 1–41.

[31] S.C. Dhingra, D.J. Gunn, P.V. Narayanan, The analysis of heat transfer in fixed beds of particles at low and intermediate Reynolds numbers, International Journal of Heat and Mass Transfer 27 (1984) 2377–2385.